



HAL
open science

Multiple nutritional strategies of hydrothermal vent shrimp (*Rimicaris hybisae*) assemblages at the Mid-Cayman Rise

Emma A.A. Versteegh, Cindy L. van Dover, Loic van Audenhaege, Max Coleman

► **To cite this version:**

Emma A.A. Versteegh, Cindy L. van Dover, Loic van Audenhaege, Max Coleman. Multiple nutritional strategies of hydrothermal vent shrimp (*Rimicaris hybisae*) assemblages at the Mid-Cayman Rise. *Deep Sea Research Part I: Oceanographic Research Papers*, 2023, 192, 103915 (8p.). 10.1016/j.dsr.2022.103915 . hal-04203913

HAL Id: hal-04203913

<https://hal.science/hal-04203913>

Submitted on 22 Feb 2024

HAL is a multi-disciplinary open access archive for the deposit and dissemination of scientific research documents, whether they are published or not. The documents may come from teaching and research institutions in France or abroad, or from public or private research centers.

L'archive ouverte pluridisciplinaire **HAL**, est destinée au dépôt et à la diffusion de documents scientifiques de niveau recherche, publiés ou non, émanant des établissements d'enseignement et de recherche français ou étrangers, des laboratoires publics ou privés.



Multiple nutritional strategies of hydrothermal vent shrimp (*Rimicaris hybisae*) assemblages at the Mid-Cayman Rise

Emma A.A. Versteegh^{a,*}, Cindy L. Van Dover^b, Loïc Van Audenhaege^c, Max Coleman^a

^a NASA Jet Propulsion Laboratory, California Institute of Technology, 4800 Oak Grove Drive, Pasadena, CA, 91109, USA

^b Division of Marine Science and Conservation, Nicholas School of the Environment, Duke University, 135 Marine Lab Road, Beaufort, NC, 28516, USA

^c Univ Brest, CNRS, Ifremer, UMR6197 BEEP, F-29280, Plouzané, France

ARTICLE INFO

Keywords:

Carbon isotopes
Gut content
Nitrogen isotopes
Sulfur isotopes
Von Damm Vent field

ABSTRACT

Alvinocaridid shrimp occurring in dense assemblages close to vigorously venting orifices are characteristic of many vent fields on the Mid-Atlantic Ridge, Central Indian Ridge, and Mid-Cayman Rise. Episymbiotic bacteria of these shrimp are exposed to vent fluids enriched in inorganic nutrients (carbon dioxide, sulfide) that, together with dissolved oxygen in the surrounding seawater, sustain autotrophic growth and supply nourishment to the shrimp. Enigmatically, conspecific shrimp may also be found sparsely distributed in the periphery of a vent field, where there is little visual evidence of vent fluid flux. We tested the null hypothesis that nourishment sources were identical for the central (dense) and peripheral shrimp assemblages, using gut content and stable isotope analyses. *Rimicaris hybisae* were sampled from central and peripheral assemblages at the Von Damm Vent Field (Mid-Cayman Rise). Guts of centrally aggregated shrimp contained a white material inferred to be bacteria, while peripheral individuals contained this white material and/or pieces of crustacean exoskeletons. C, N, and S isotopic compositions of shrimp muscle tissues were significantly different between central and peripheral shrimp assemblages, and little overlap in isotopic space was found. A comparison of $\delta^{13}\text{C}$ and $\delta^{34}\text{S}$ values of gut contents and abdominal tissues revealed that abdominal tissue composition reflects the shrimp's source of nourishment. Slight but significantly elevated $\delta^{15}\text{N}$ values in peripheral shrimp, together with crustacean exoskeleton fragments in the gut, suggest facultative carnivory in peripherally aggregated shrimp. The lower $\delta^{13}\text{C}$ and $\delta^{34}\text{S}$ values in individuals from the peripheral assemblages are also consistent with a mixotrophic diet. We conclude that central and peripheral assemblages of *R. hybisae* have different nourishment sources, with central assemblages relying on episyntons, while peripheral assemblages have diverse nourishment sources comprising bacteria and Crustacea.

1. Introduction

Although the existence of chemoautotrophic pathways had been suggested in the 1880s (Winogradsky, 1887), the importance of chemosynthetic bacteria as the base of entire food webs only became evident with the discovery of deep-sea hydrothermal vents and the high-biomass faunal communities around them (Cavanaugh et al., 1981; Corliss et al., 1979; Lonsdale, 1977). Free-living as well as symbiotic bacterial communities use the energy from oxidation of reduced compounds in the hydrothermal fluids (e.g. H_2 , H_2S , CH_4) to fix CO_2 into organic carbon.

Along the ultra-slow spreading Mid-Cayman Rise (MCR), two hydrothermal vent fields were discovered in 2010: the Piccard Vent Field, the world's deepest at ~ 4960 m, and the shallower Von Damm Vent Field at ~ 2300 m (Connelly et al., 2012; German et al., 2010). The Piccard Vent Field is located in the rift valley of the MCR with high temperature (354–398 °C) black smoker venting and some diffuse venting at lower temperatures (111 °C). Von Damm is an off-axis vent field, located on the upper slopes of an oceanic core complex, with high-temperature (232 °C) diffuse venting (Kinsey and German, 2013).

At both sites, dense aggregations of the alvinocaridid shrimp *Rimicaris hybisae* occur, occupying 100% of rock surfaces several layers thick,

* Corresponding author.

E-mail addresses: e.a.versteegh@hr.nl (E.A.A. Versteegh), clv3@duke.edu (C.L. Van Dover), lvanaude@ifremer.fr (L. Van Audenhaege), max.coleman@jpl.nasa.gov (M. Coleman).

¹ Present address: Utrecht University, Freudenthal Institute, Princetonplein 5 3584CC Utrecht, e.a.a.versteegh@uu.nl

² Present address: Rotterdam University of Applied Sciences, School of Education, Museumplein 40, 3015CX Rotterdam, the Netherlands, e.a.a.versteegh@hr.nl

<https://doi.org/10.1016/j.dsr.2022.103915>

Received 26 August 2022; Received in revised form 24 October 2022; Accepted 26 October 2022

Available online 2 November 2022

0967-0637/© 2022 The Authors. Published by Elsevier Ltd. This is an open access article under the CC BY license (<http://creativecommons.org/licenses/by/4.0/>).

around actively venting orifices (Fig. 1a; Connelly et al., 2012; Nye et al., 2012; Plouviez et al., 2015). At Von Damm we observed that peripheral to the dense aggregations and away from active venting, the same species occurs much more sparsely distributed, covering less than 10% of the rock surface (Fig. 1b). The dense aggregations around active venting are hereafter referred to as “central assemblages”, the sparse aggregations away from active venting are hereafter referred to as “peripheral assemblages”.

R. hybisae exhibits high spatial variability in sex ratios, population structure, size, and development of oocytes and embryos, which is probably caused by environmental variables and might be related to the observed central/peripheral distributions (Nye et al., 2013b). Central assemblages at Von Damm and Piccard have a female-biased sex ratio. However, when ovigerous females were excluded, there was no significant deviation from a 1:1 sex ratio (Nye et al., 2013b).

Similarly, central and peripheral assemblages have been described for the related Mid-Atlantic Ridge (MAR) species *Rimicaris exoculata*, which can be considered an analog for *R. hybisae* at MCR. Copley et al. (1997) suggested that dense assemblages reflect local availability of substratum exposed to the flow of hydrothermal fluids. In contradiction to *R. hybisae*, it has been found that in *R. exoculata* females dominate dense swarms near active venting, while males are sparsely distributed in the periphery (Hernández-Ávila et al., 2022; Methou et al., 2022; Vinogradov and Vereshchaka, 1995).

R. hybisae has an enlarged cephalothorax harboring epibiotic bacteria, on which it predominantly relies for its organic carbon (Nye et al., 2012; Streit et al., 2015). The bacterial communities are different between Von Damm and Piccard, but similar to free-living bacterial profiles of the local environment (Assié, 2016). *R. hybisae* at Von Damm has similar bacterial population profiles as *R. exoculata* at Logatchev (MAR), possibly reflecting the geochemical and physical similarity of the sites (ultramafic, depth \pm 2500 m; Assié, 2016).

Biology of *R. exoculata* has been extensively discussed in Zbinden and Cambon-Bonavita (2020). This species is considered a primary consumer (Segonzac et al., 1993) and was initially thought to graze on bacteria associated with minerals of black-smoker chimneys (Van Dover et al., 1988). It is now clear that *R. exoculata* harbors various types of symbiotic bacteria in its enlarged gill chambers, on its mouthparts, and in its gut (Colaço et al., 2007; Durand et al., 2009; Jan et al., 2014; Polz et al., 1998; Ponsard et al., 2013; Zbinden and Cambon-Bonavita, 2003; Zbinden et al., 2008). These epibionts provide the major food source for *R. exoculata*, rather than free-living bacteria on chimney walls (Gebruk et al., 2000; Pond et al., 1997; Rieley et al., 1999). The epibiont bacteria

use various chemoautotrophic pathways, such as iron, sulfide and methane oxidation, and potentially hydrogen oxidation (Hügler et al., 2011; Petersen et al., 2011; Zbinden et al., 2008). A few publications report additional potential food sources for *R. exoculata*. Segonzac et al. (1993) found parts of Crustacea in a *R. exoculata* stomach, and ascribed this to accidental ingestion of a copepod while grazing on bacterial mats. Ponsard et al. (2013) found that the *R. exoculata* acquires dissolved organic carbon from their epibionts by permeation across the gill chamber integument. Apremont et al. (2018) suggested *Rimicaris chacei* (discussed hereafter) acquires some of its organic carbon the same way.

According to genetic markers, *R. hybisae* is most closely related to the MAR species *Rimicaris chacei* and might even belong to the same species (Plouviez et al., 2015; Teixeira et al., 2013; Vereshchaka et al., 2015). *R. chacei*, however, may occupy a slightly different niche than *R. hybisae*; it occurs only in peripheral populations away from active vents and acquires food by scavenging or predation, while also depending on epibiotic bacteria (Apremont et al., 2018; Gebruk et al., 2000; Methou et al., 2020, 2022). *R. chacei* has microbial communities in the same locations as *R. exoculata* (mouthparts, gill chamber and gut), consisting of a variety of bacterial groups, closely related to those in *R. exoculata* (Apremont et al., 2018; Cowart et al., 2017; Durand et al., 2009, 2015; Zbinden and Cambon-Bonavita, 2003; Zbinden et al., 2008).

Stable isotopes of carbon ($\delta^{13}\text{C}$ values) and nitrogen ($\delta^{15}\text{N}$ values) are useful tools in determining trophic positions and disentangling food webs. Generally, an animal's tissues are enriched by about 1‰ in $\delta^{13}\text{C}$ values and about 3.4‰ in $\delta^{15}\text{N}$ values relative to its diet (DeNiro and Epstein, 1978; Minagawa and Wada, 1984). Sulfur stable isotopic compositions ($\delta^{34}\text{S}$ values) have been less studied, but also appear to be slightly enriched with each trophic step (McCutchan et al., 2003). In chemoautotrophic ecosystems, $\delta^{34}\text{S}$ values are generally lower for thiotrophs than for other groups, e.g. methanotrophs (Vetter and Fry, 1998).

Several studies have examined stable isotopic compositions in four *Rimicaris* species (Table 1). Within a species, stable isotopic compositions are found to differ between vent fields (Colaço et al., 2002; Gebruk et al., 2000). Vereshchaka et al. (2000) compared central and peripheral assemblages in *R. exoculata* and found that the peripheral individuals had lower $\delta^{13}\text{C}$ values and higher $\delta^{15}\text{N}$ values than the central shrimp. They attributed the difference to ontological changes from juveniles (peripheral) having a greater photosynthetic source of diet than the central, adult population, which is dominated by chemosynthetic nourishment. Such ontogenetic shifts in nourishment source and

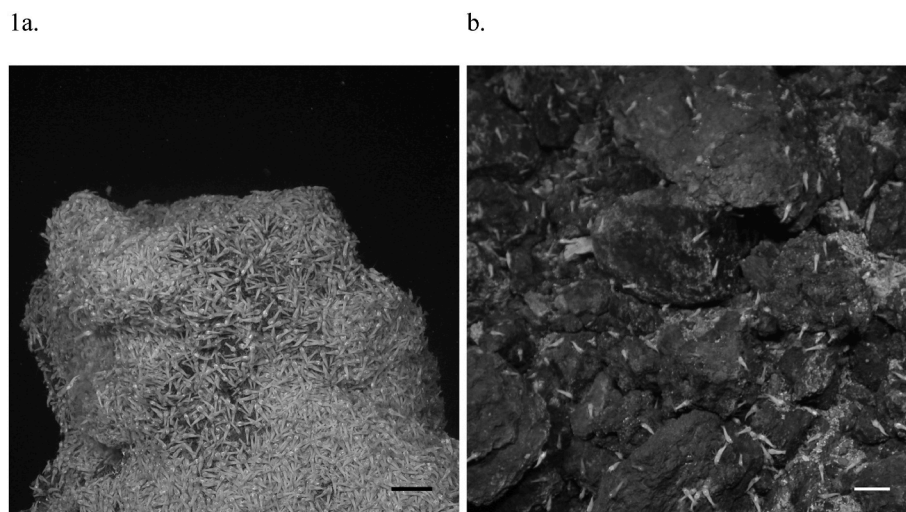


Fig. 1. a. Central assemblage of *R. hybisae* on the Von Damm spire; b. Peripheral assemblage of *R. hybisae* at Von Damm; scale bars are 10 cm. Pictures taken during the R/V Atlantis Oases 2012 cruise by the ROV Jason, Woods Hole Oceanographic Institution.

Table 1
Published stable isotope values of body tissues of adult specimens for 4 species in the genus *Rimicaris*.

Species	Location	Field	Tissue type	$\delta^{13}\text{C}$ (VPDB)					$\delta^{15}\text{N}$ (AIR)					$\delta^{34}\text{S}$ (VCDT)					Reference	
				Min	Max	Mean	SD	n	Min	Max	Mean	SD	n	Min	Max	Mean	SD	n		
<i>Rimicaris chacei</i>	MAR	Broken Spur	Muscle	-14.54	-13.96	-14.25	0.41	2			7.59		1							Colaço et al. (2002)
<i>Rimicaris chacei</i>	MAR	Broken Spur	Abdominal muscle	-13.61	-13.02	-13.32	0.42	2	7.98	8.00	7.99	0.01	2							Gebruk et al. (2000)
<i>Rimicaris chacei</i>	MAR	Broken Spur	20 whole individuals			-13.9		20											Vereshchaka et al. (2000)	
<i>Rimicaris chacei</i>	MAR	Logatchev	Abdominal muscle			-13.28		1			7.71		1						Gebruk et al. (2000)	
<i>Rimicaris chacei</i>	MAR	Lucky Strike	Muscle	-16.14	-12.32	-14.55	1.22	12	2.94	6.46	4.88	1.39	6						Colaço et al. (2002)	
<i>Rimicaris chacei</i>	MAR	Lucky Strike	Abdominal muscle	-15.14	-11.67	-13.47	1.22	9	4.75	7.31	6.04	0.89	9						Gebruk et al. (2000)	
<i>Rimicaris chacei</i>	MAR	Snake Pit	Abdominal muscle			-13.44		1			8.03		1						Gebruk et al. (2000)	
<i>Rimicaris chacei</i>	MAR	Snake Pit	Abdominal muscle	-19.00	-11.40	-15.67	2.08	18	4.30	8.70	6.50	1.24	18	4.2	11.6	8.53	1.83	18	Methou et al. (2020)	
<i>Rimicaris chacei</i>	MAR	TAG	Abdominal muscle			-15.56		1			7.32		1						Gebruk et al. (2000)	
<i>Rimicaris chacei</i>	MAR	TAG	Abdominal muscle	-18.70	-13.70	-15.72	1.09	33	6.00	9.50	8.06	1.10	33	14.1	9.3	11.35	1.21	33	Methou et al. (2020)	
<i>Rimicaris exoculata</i>	MAR	Broken Spur	Muscle	-17.34	-10.00	-12.76	2.77	5	5.72	6.99	6.42	0.54	5						Colaço et al. (2002)	
<i>Rimicaris exoculata</i>	MAR	Broken Spur	Abdominal muscle	-14.55	-10.75	-12.65	2.69	2	6.18	7.64	6.91	1.03	2						Gebruk et al. (2000)	
<i>Rimicaris exoculata</i>	MAR	Logatchev	Muscle	-15.97	-12.25	-14.43	2.03	4	5.87	8.02	6.94	1.52	2						Colaço et al. (2002)	
<i>Rimicaris exoculata</i>	MAR	Logatchev	Abdominal muscle			-14.44		1			5.84		1						Gebruk et al. (2000)	
<i>Rimicaris exoculata</i>	MAR	Lucky Strike	Muscle			-12.11		1			7.85		1						Colaço et al. (2002)	
<i>Rimicaris exoculata</i>	MAR	Lucky Strike	Abdominal muscle	-11.13	-11.10	-11.12	0.02	2	7.45	7.87	7.66	0.30	2						Gebruk et al. (2000)	
<i>Rimicaris exoculata</i>	MAR	Rainbow	Muscle	-17.04	-8.29	-10.21	2.08	32	5.76	8.11	6.80	0.63	19						Colaço et al. (2002)	
<i>Rimicaris exoculata</i>	MAR	Rainbow	Abdominal muscle	-10.09	-9.97	-10.03	0.08	2	7.43	7.98	7.71	0.39	2						Gebruk et al. (2000)	
<i>Rimicaris exoculata</i>	MAR	Snake Pit	Muscle	-15.15	-10.70	-12.77	1.66	7	4.72	7.30	6.12	0.87	7						Colaço et al. (2002)	
<i>Rimicaris exoculata</i>	MAR	Snake Pit	Abdominal muscle	-13.84	-12.05	-12.86	0.91	3	5.93	6.88	6.30	0.51	3						Gebruk et al. (2000)	
<i>Rimicaris exoculata</i>	MAR	Snake Pit	Abdominal muscle	-12.90	-11.20	-11.85	0.41	26	6.80	8.30	7.43	0.38	26	5.5	9.8	7.85	1.23	26	Methou et al. (2020)	
<i>Rimicaris exoculata</i>	MAR	Snake Pit	Abdominal muscle	-14.9	-13.5	-14.0	0.6	10	5.4	6.3	5.7	0.3	10						Polz et al. (1998)	
<i>Rimicaris exoculata</i>	MAR	TAG	Muscle	-15.98	-11.77	-14.28	1.87	5	3.83	7.02	5.58	1.06	4						Colaço et al. (2002)	
<i>Rimicaris exoculata</i>	MAR	TAG	Abdominal muscle	-11.47	-11.05	-11.26	0.30	2	5.55	6.57	6.06	0.72	2						Gebruk et al. (2000)	
<i>Rimicaris exoculata</i>	MAR	TAG	Abdominal muscle	-13.10	-12.00	-12.49	0.28	30	6.60	7.50	7.13	0.25	30	6.4	9.7	8.53	0.66	30	Methou et al. (2020)	
<i>Rimicaris exoculata</i>	MAR	TAG	Abdominal muscle	-12.1	-11.6	-11.9	0.4	2	7.5	7.7	7.6	0.1	2			9.7		5	Van Dover et al. (1988)	
<i>Rimicaris exoculata</i> central	MAR	Broken Spur	20 whole individuals			-9.8		20			5.50		20						Vereshchaka et al. (2000)	
<i>Rimicaris exoculata</i> peripheral	MAR	Broken Spur	20 whole individuals			-10.9		20			7.00		20						Vereshchaka et al. (2000)	
<i>Rimicaris</i> sp.	MAR	Snake Pit	Abdominal muscle	-16.9	-15.2	-15.8	0.6	10	4.5	5.3	4.9	0.2	10						Polz et al. (1998)	
<i>Rimicaris kairei</i>	CIR	Kairei	Muscle	-13.5	-12.2	-12.8	0.5	7	6.5	7.7	7.1	0.4	7						Van Dover (2002)	
<i>Rimicaris</i> sp.	CIR	OVF	Muscle			-14.60	1.10	6			7.40	1.80	6			7.90	1.70	6	Suh et al. (2022)	
<i>Rimicaris hybisae</i>	MCR	Piccard	Muscle	-12.52	-10.13	-11.37	0.72	10	5.92	8.92	7.02	0.83	11	10.81	11.14	10.98	0.23	2	Bennett et al. (2015)	
<i>Rimicaris hybisae</i>	MCR	Von Damm	Muscle	-22.68	-12.25	-14.39	2.84	18	4.97	8.85	6.24	0.90	24	12.23	14.50	13.06	0.67	12	Bennett et al. (2015)	
<i>Rimicaris hybisae</i> central	MCR	Von Damm	Abdominal muscle	-16.44	-13.16	-14.45	1.03	19	7.10	8.13	7.56	0.29	11	11.82	14.68	13.09	0.		This study	
<i>Rimicaris hybisae</i> peripheral	MCR	Von Damm	Abdominal muscle	-19.35	-13.72	-16.77	1.99	11	7.53	8.78	7.92	0.37	11	7.70	13.15	10.71	1.85	11	This study	

isotopic composition have indeed been described in *R. exoculata* (Gebbruk et al., 2000; Methou et al., 2022), *R. chacei* (Methou et al., 2020), as well as *Rimicaris kairei* (Central Indian Ridge (CIR); Suh et al., 2022; Van Dover, 2002). $\delta^{15}\text{N}$ values of *R. chacei* ranged from 2.94 to 9.50‰, reflecting the fact that they can be facultatively carnivorous/scavengers (Colaço et al., 2002; Gebbruk et al., 2000; Methou et al., 2020).

Initial work on *R. hybisae* at the Piccard Vent Field yielded $\delta^{13}\text{C}$ values of -12.5 to -10.1 ‰, $\delta^{15}\text{N}$ values of 5.9–8.9‰ and $\delta^{34}\text{S}$ values ranging from 10.8 to 11.1‰, while the Von Damm Vent Field $\delta^{13}\text{C}$ values ranged from -22.7 to -12.3 ‰, $\delta^{15}\text{N}$ values of 5.0–8.9‰ and $\delta^{34}\text{S}$ values of 12.2–14.8‰ (Bennett et al., 2015). When compared with isotopic compositions of the primary producers and other consumers in the food web, $\delta^{15}\text{N}$ values indicate that *R. hybisae* is a primary consumer of chemoautotrophic organic material. The range in $\delta^{13}\text{C}$ values, was only 2.4‰ at the Piccard Vent Field, but 10.4‰ at the Von Damm Vent Field. The large range of $\delta^{13}\text{C}$ values at the Von Damm Vent Field led to the assumption that $\delta^{13}\text{C}$ values are not a useful tool in studying trophic relations at hydrothermal vents (Bennett et al., 2015), since they may result from mixtures of different types of chemoautotrophy, e.g. methanotrophy vs. thiotrophy (Kennicutt et al., 1992; Leonard et al., 2021). We hypothesize, however, that they might instead be related to size or spatial distribution (central or peripheral to active venting). Variation in $\delta^{34}\text{S}$ values are assumed to reflect local vent fluid $\delta^{34}\text{S}$ values and related differences in chemosynthetic bacterial assemblages (Bennett et al., 2015).

The occurrence of conspecific shrimp assemblages in close proximity at the Von Damm Vent Field, gave us a natural test bed to investigate nourishment sources and trophic positions of *R. hybisae* assemblages central and peripheral to active venting. We set out to answer the following questions:

1. To what extent do central and peripheral assemblages differ in gut contents, in $\delta^{13}\text{C}$, $\delta^{15}\text{N}$ and $\delta^{34}\text{S}$ values, and in the volume of isotopic trait space they occupy?
2. From isotopic data and gut contents, can we infer nourishment sources of central and peripheral *R. hybisae* assemblages?

2. Materials and methods

2.1. Sample collection

Samples were collected at the Von Damm vent field (18°23'N; 81°48'W; 2309 m) on August 26, 2013 using the remotely operated vehicle (ROV) *Hercules* during the *E/V Nautilus* Expedition, led by C. German (Woods Hole Oceanographic Institution). *R. hybisae* were collected by a multi-chamber slurp pump to ensure samples were not cross-contaminated. Central shrimp assemblages were collected from the Von Damm spire (Fig. 1a) near vigorous venting (>15 °C); peripheral shrimp assemblages were collected on a separate dive from an area of weakly diffusing fluids (<21 °C; see also Plouviez et al., 2015), 1 m away from the central shrimp assemblages. Immediately after collection, carapace length (end tail to tip of rostrum) was measured with a caliper and individuals were dissected and gut contents identified (white material inferred to be of bacterial origin, herein referred to as “bacteria”/crustacean exoskeleton/empty). In total 39 individual *R. hybisae* were collected, of which 30 abdominal tissue samples and 25 matching gut content samples were obtained. All samples were frozen separately at -20 °C until further analysis. On shore, all samples were frozen at -80 °C and freeze-dried. Abdominal tissue samples were homogenized with a pestle and mortar.

2.2. Isotopic analyses

Samples were weighed into tin capsules and analyzed using a combined method for $\delta^{13}\text{C}$ and $\delta^{15}\text{N}$ values and a separate setup for $\delta^{34}\text{S}$

values on a Thermo Scientific (Waltham MA, USA) MAT 253 isotope ratio mass spectrometer, connected to a Costech Analytical (Valencia CA, USA) ECS 4010 elemental analyzer.

$\delta^{13}\text{C}$ values were calibrated using international standards NBS-18 and NBS-19, and expressed against Vienna Pee Dee Belemnite (VPDB). The long-term reproducibility (1σ) of a routinely analyzed acetanilide lab standard was <0.05 ‰. $\delta^{15}\text{N}$ values were expressed against atmospheric N_2 and calibrated using international standards IAEA-N1 and IAEA-N2. Long-term reproducibility (1σ) of the acetanilide lab standard was <0.1 ‰. $\delta^{34}\text{S}$ values were expressed against Vienna Cañon Diablo Troilite (VCDT), and calibrated using elemental S, BaSO_4 and Ag_2S lab standards. Lab standard $\delta^{34}\text{S}$ values were verified against international standards IAEA-S/1, NBS-127, NIST-8553 and NIST-8455. Reproducibility (1σ) of routinely analyzed lab standards was <0.4 ‰ for sulfanilamide, <0.3 ‰ for Ag_2S , and <0.2 ‰ for elemental S and BaSO_4 .

All abdominal tissue samples were analyzed in duplicate or triplicate. Gut content samples ($n = 25$ of which 21 were successfully analyzed) were individually analyzed for $\delta^{13}\text{C}$ and $\delta^{15}\text{N}$ values ($n = 17$) and/or $\delta^{34}\text{S}$ values ($n = 10$). Because of their small mass a few gut content samples were pooled for $\delta^{34}\text{S}$ analysis, resulting in 2 additional $\delta^{34}\text{S}$ values.

2.3. Statistical analyses

All analyses were done using R (R Core Team, 2013).

A Kruskal-Wallis test was performed with abdominal isotopic compositions ($\delta^{13}\text{C}_{\text{abd}}$, $\delta^{15}\text{N}_{\text{abd}}$, $\delta^{34}\text{S}_{\text{abd}}$ values) as dependent variables and by the following factors: assemblage (central/peripheral), gut content bacteria (present/absent), and gut content crustacea (present/absent).

We tested the effect of individual length on abdominal isotopic signature by computing the significance of the slope of a linear regression.

To explore differences in isotopic trait space occupied by central and peripheral assemblages, 2D isotope plots with convex hulls were constructed (Cornwell et al., 2006). Further comparison of the isotopic trait spaces was done by calculating two overlap metrics: isotopic similarity (ISim) and isotopic nestedness (INes). ISim is the ratio between the volume of the intersection and the volume of the union of the two assemblages in isotope space. ISim ranges from 0 (when the two assemblages fill entirely different parts of isotope space) to 1 (when they fill the same portion of isotope space). INes is the ratio between the volume of the intersection and the minimal volume filled by a group. It ranges from 0 (no isotopic overlap) to 1 when one assemblage fills a subset of the isotopic space filled by the other assemblage (Cucherousset and Villéger, 2015; Villéger et al., 2011). We tested for difference in centroid locations in the $\delta^{13}\text{C}_{\text{abd}}-\delta^{15}\text{N}_{\text{abd}}-\delta^{34}\text{S}_{\text{abd}}$ isotopic space between peripheral and central assemblages using a residual permutation procedure ($n = 999$; Turner et al., 2010).

The relationship between gut content and abdominal tissue isotopic compositions was determined using a linear regression.

3. Results

3.1. Gut contents

Gut contents of most shrimp (17 of 19 individuals) from central assemblages at the Von Damm vent field consisted of white, amorphous material, which was macroscopically inferred to be bacteria, analogous to the gut contents of other *Rimicaris* species (Apremont et al., 2018; Durand et al., 2009, 2015). Two individuals had empty guts and the gut of one individual contained a small bit of crustacean exoskeleton in addition to bacteria.

Peripheral shrimp (~ 1 m from central assemblages; $n = 20$) had guts filled with fragments of crustacean exoskeleton (5 individuals), a mixture of bacteria and crustacean exoskeleton (3 individuals), or bacteria only (6 individuals). Six individuals had empty guts.

A Kruskal-Wallis test confirms that centrally aggregated shrimp more often have bacteria in their gut ($\chi^2 = 5.410$, $p = 0.020$), while fragments of crustacean exoskeleton are more often found in the guts of peripheral shrimp ($\chi^2 = 11.715$, $p = 0.001$).

3.2. Isotopic composition of shrimp abdominal tissues

As expected, the ranges and averages of *Rimicaris hybisae* $\delta^{13}\text{C}_{\text{abd}}$, $\delta^{15}\text{N}_{\text{abd}}$, $\delta^{34}\text{S}_{\text{abd}}$ values were similar to those previously reported in the same species from the Von Damm Vent Field (Bennett et al., 2015, Table 1).

There was no significant linear relationship between carapace length and $\delta^{13}\text{C}_{\text{abd}}$, $\delta^{15}\text{N}_{\text{abd}}$, $\delta^{34}\text{S}_{\text{abd}}$ values.

However, when isotopic compositions of abdominal tissue of individuals from central and peripheral assemblages were compared (Kruskal-Wallis test), significant distinctions were resolved: $\delta^{13}\text{C}_{\text{abd}}$ values of peripheral *R. hybisae* (-19.4 to -13.7‰) were on average 2.4‰ lower than $\delta^{13}\text{C}_{\text{abd}}$ values for central individuals (-16.4 to -13.2‰ vs. VPDB; $\chi^2 = 8.946$, $p = 0.003$; Fig. 2). $\delta^{15}\text{N}_{\text{abd}}$ values fell in a narrow range and were elevated by 0.3‰ in peripheral shrimp (7.5 – 8.8‰) in comparison to centrally aggregated individuals (7.1 – 8.1‰ ; $\chi^2 = 6.903$, $p = 0.009$; Fig. 2). $\delta^{34}\text{S}_{\text{abd}}$ values of peripheral shrimp (7.7 – 13.2‰) were on average 2.2‰ lower than those of centrally aggregated shrimp (11.8 – 14.7‰ ; $\chi^2 = 10.700$, $p = 0.001$; Fig. 2; see Table 1 for means and σ values).

In order to quantify the overlap of central and peripheral assemblages in isotopic space, 2D convex hulls were determined (Fig. 2) and ISim and INes were calculated for each stable isotope axis separately and in 2D and 3D space. Central and peripheral assemblages overlap in 2D isotope trait space, but only to a limited degree (Table 2). In 3D isotope trait space there is hardly any overlap (ISim = 0.01), but this is due to a single sample that has a large influence on the convex hull extent. When excluding this sample, there is no overlap (ISim = 0) for central and peripheral assemblages in 3D isotope trait space.

Difference in centroid locations in the 3D isotopic space among peripheral and central assemblages was significant ($p = 0.001$).

3.3. Isotopic composition of *R. hybisae* gut contents

To determine if the isotopic values of *R. hybisae* tissues reflect their sources of nourishment, within-individual values for gut contents and abdominal tissue were compared by means of linear regression. A positive relationship between the $\delta^{13}\text{C}$ value of gut contents ($\delta^{13}\text{C}_{\text{gut}}$) of an

Table 2

Isotopic similarity (ISim) and isotopic nestedness (INes) for all carbon, nitrogen, and sulfur isotopic compositions of central and peripheral assemblages of *R. hybisae* at Von Damm Vent Field.

Isotope space	ISim	INes
$\delta^{13}\text{C}$	0.44	0.83
$\delta^{15}\text{N}$	0.37	0.61
$\delta^{34}\text{S}$	0.20	0.54
$\delta^{13}\text{C}/\delta^{15}\text{N}$	0.18	0.36
$\delta^{13}\text{C}/\delta^{34}\text{S}$	0.12	0.38
$\delta^{15}\text{N}/\delta^{34}\text{S}$	0.05	0.16
$\delta^{13}\text{C}/\delta^{15}\text{N}/\delta^{34}\text{S}$	0.01	0.05

individual (consumption at a point in time) and the $\delta^{13}\text{C}_{\text{abd}}$ value of the same individual (nourishment integrated over a longer period) was observed ($R^2 = 0.755$, $p < 0.001$, $df = 14$; Fig. 3a). Similarly, there was a positive relationship between within-individual $\delta^{34}\text{S}_{\text{gut}}$ and $\delta^{34}\text{S}_{\text{abd}}$ values ($R^2 = 0.543$, $p = 0.015$, $df = 9$; Fig. 3c). There was no significant relationship between $\delta^{15}\text{N}_{\text{abd}}$ and gut content $\delta^{15}\text{N}$ ($\delta^{15}\text{N}_{\text{gut}}$) values (Fig. 3b).

To estimate the amount of trophic enrichment between gut content and abdominal tissue, the intercept of the Y-axis was calculated when a line with slope 1 was forced through the data. This shows there was no enrichment between $\delta^{13}\text{C}_{\text{gut}}$ and $\delta^{13}\text{C}_{\text{abd}}$ values (-0.08‰) or between $\delta^{34}\text{S}_{\text{gut}}$ and $\delta^{34}\text{S}_{\text{abd}}$ values (-0.49‰). The enrichment between $\delta^{15}\text{N}_{\text{gut}}$ and $\delta^{15}\text{N}_{\text{abd}}$ values was on average 3.35‰ .

4. Discussion

The examination of the gut contents of peripheral and central assemblages of *R. hybisae* showed that they had different sources of nourishment. It appears that centrally aggregated shrimp use only their epibiotic bacteria as a food source, whereas peripheral individuals rely on small Crustacea, epibiotic bacteria, or both. By analogy with *R. exoculata*, it seems likely that the presence of bacteria in the gut indicates a primary bacterial chemosynthetic source of nourishment and that there would be a much larger contribution from the gill chamber epibionts (Ponsard et al., 2013).

Gut content and abdominal tissue had similar $\delta^{13}\text{C}$ and $\delta^{34}\text{S}$ values (no isotopic enrichment), suggesting that the gut contents can serve as indicators of the integrated nourishment sources of the individual and not just as a consumption at a given moment. The within-individual comparison of the $\delta^{15}\text{N}$ values of gut contents versus abdominal tissues revealed the expected isotopic shift of one trophic level ($+3.4\text{‰}$;

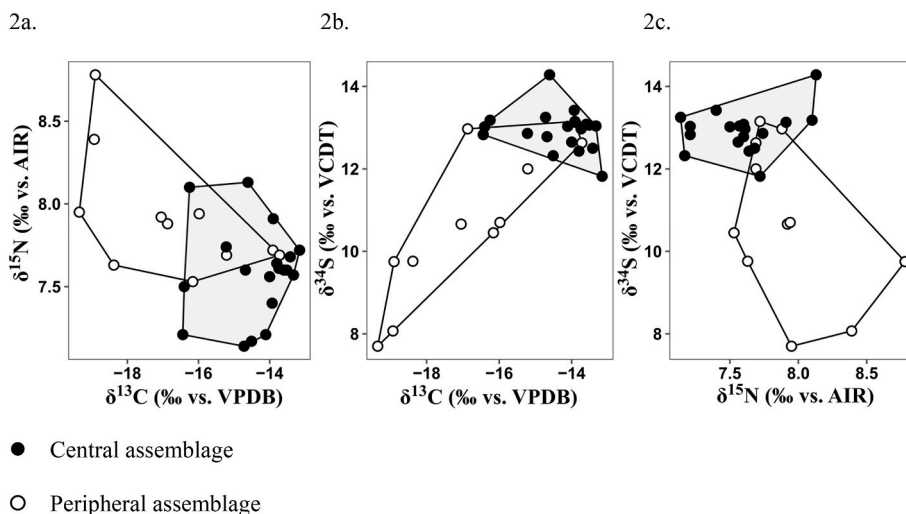


Fig. 2. a-c. Biplots of $\delta^{13}\text{C}$, $\delta^{15}\text{N}$ and $\delta^{34}\text{S}$ values of *R. hybisae* abdominal tissues with enclosing convex hulls in $\delta^{13}\text{C}/\delta^{15}\text{N}$, $\delta^{13}\text{C}/\delta^{34}\text{S}$ and $\delta^{15}\text{N}/\delta^{34}\text{S}$ isotopic trait space. Standard deviations on duplicate measurements were $< 0.2\text{‰}$ for $\delta^{13}\text{C}$ and $\delta^{15}\text{N}$ values and $< 0.4\text{‰}$ for $\delta^{34}\text{S}$ values.

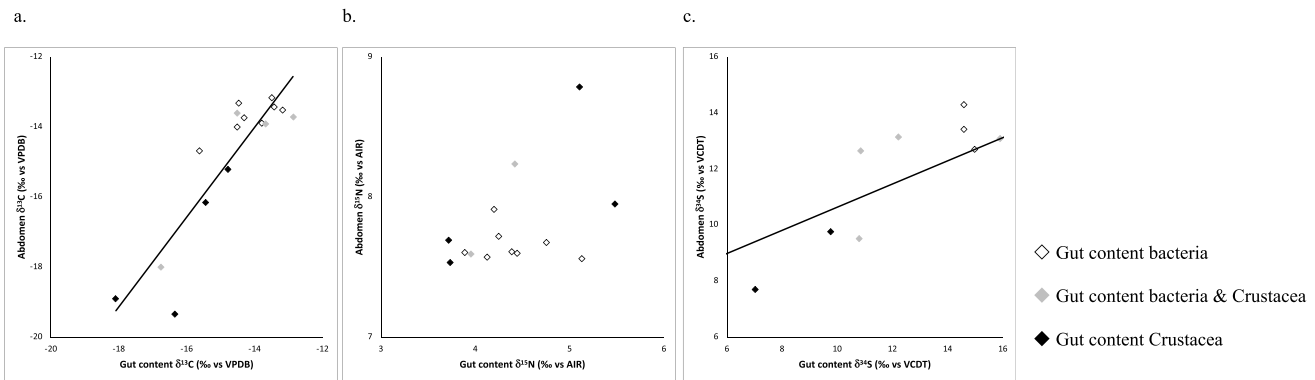


Fig. 3. a. Relationship between $\delta^{13}\text{C}$ values of *R. hybisae* gut contents and abdominal tissues, described by $\delta^{13}\text{C}_{\text{abd}} = 1.244 \times \delta^{13}\text{C}_{\text{gut}} + 3.405$ ($R^2 = 0.755$, $p < 0.001$, $df = 14$); b. Comparison of $\delta^{15}\text{N}$ values of *R. hybisae* gut contents and abdominal tissues; c. Relationship between $\delta^{34}\text{S}$ values of *R. hybisae* gut contents and abdominal tissues, described by $\delta^{34}\text{S}_{\text{abd}} = 0.414 \times \delta^{34}\text{S}_{\text{gut}} + 6.491$ ($R^2 = 0.543$, $p = 0.015$, $df = 9$). 1σ errors on duplicate measurements were $< 0.6\text{‰}$ for $\delta^{13}\text{C}$ and $\delta^{15}\text{N}$ values and $< 0.7\text{‰}$ for $\delta^{34}\text{S}$ values.

Minagawa and Wada, 1984; Vander Zanden and Rasmussen, 2001), i.e. a 3.35‰ enrichment in $\delta^{15}\text{N}$ values. This finding, however, is uncertain as the relationship between gut content and abdominal tissue $\delta^{15}\text{N}$ values was not significant.

$\delta^{15}\text{N}_{\text{abd}}$ values of centrally aggregated *R. hybisae* were only enriched by 0.3‰ in comparison to peripheral individuals, suggesting that the different nourishment sources of central and peripheral individuals did not comprise a difference of an entire trophic level (bacterially sourced nutrition vs. carnivore). It is possible that trans-tegumental absorption of nutrients (primarily from the gill chambers; Ponsard et al., 2013) might affect the observed change with trophic level, as this would potentially cause less isotopic fractionation than a series of reactions in a metabolic pathway as would be used by ingestion of bacteria.

The significantly lower $\delta^{13}\text{C}_{\text{abd}}$ and $\delta^{34}\text{S}_{\text{abd}}$ values in peripheral shrimp compared to centrally aggregated shrimp could have several causes. Methou et al. (2022) observed in *R. exoculata* that peripheral aggregations consisted mostly of juveniles which may have had a different nourishment source than adults. Our samples, however, only comprised individuals of adult size. Lower $\delta^{13}\text{C}$ and $\delta^{34}\text{S}$ values were found in certain potential food sources for *R. hybisae* at Cayman vents, such as the shrimp *Alvinocarid* sp. and the gastropod *Itheyaspira bathycodon* (Bennett et al., 2015; Nye et al., 2013a). These species could form part of the diet of peripheral *R. hybisae*, as the crustacean exoskeleton bits in the guts could not be identified further taxonomically, and we previously observed *R. hybisae* guts do sometimes contain gastropods. Bennett et al. (2015) suggested that varying $\delta^{34}\text{S}$ values in the food chain could be traced to differences in vent fluid chemistry through variations in species assemblages of chemosynthetic bacteria. Fluid chemistry compositions were indeed different between the central and peripheral *R. hybisae* assemblages, as the centrally aggregated shrimps were in diffuse flow fluid, while peripheral shrimp were in ambient seawater. The origin of more negative $\delta^{13}\text{C}$ and $\delta^{34}\text{S}$ values in peripheral shrimp could also be due to differences in chemosynthetic bacterial assemblages at the bottom of the food chain, given that epibiotic communities can have different microbial compositions within the same host shrimp species (Durand et al., 2009; Zbinden et al., 2008) and $\delta^{34}\text{S}$ values are more negative for thiotrophs than for other microbial groups (Vetter and Fry, 1998).

Additional causes for the observed differences in isotopic composition of shrimp abdominal tissue could be growth rates and related tissue turnover rates (Fry and Arnold, 1982; Hesselin et al., 1993), or even plausibly as different relative contributions of catabolic digestion of bacteria vs. direct supply of organic carbon compounds by symbionts to the host shrimp.

Direct comparison of stable isotope compositions, ISim and INes show limited overlap in isotopic compositions of central and peripheral

shrimp assemblages, indicating that these assemblages occupy different ecological niches. At MAR locations, similar niches are occupied by separate species (Methou et al., 2022).

It remains a mystery how two conspecific assemblages with different nutritional strategies have come to exist side by side in this manner. While isotopic compositions suggest that individuals must persist in a given habitat for some period of time, it is not clear whether shrimp ever move between peripheral and central habitats. Plouviez et al. (2015) showed that there were no genetic differences between *R. hybisae* populations at Piccard and Von Damm vent fields, or between patches of similarly-sized individuals at one location. In this light it seems plausible that central and peripheral aggregations are not genetically distinct populations, but different life history phases of the same population.

5. Conclusions

Based on the above analysis we conclude that central and peripheral assemblages of *R. hybisae* have different nourishment sources, with central assemblages relying on epibiotic bacteria while peripheral assemblages have diverse nourishment sources comprising bacteria, Crustacea, and possibly gastropods.

$\delta^{13}\text{C}$ and $\delta^{34}\text{S}$ values of abdominal tissue reflect those of gut content and are thus related to nourishment source. No significant relationship could be found for $\delta^{15}\text{N}$ values. Our findings show that tissue stable isotope compositions are effective tracers of trophic levels in hydrothermal vent food webs, despite previous doubts of their value (Bennett et al., 2015).

Future research on *R. hybisae* could address the identification of the bacteria in their guts and gill chamber integuments, as well as additional analyses of $\delta^{15}\text{N}$ values of gut contents and tissues to further elucidate the presence or absence of a relationship between them.

In addition, the questions why two groups with different nutritional strategies exist, and whether the two assemblages are indeed different life history phases of the same population remain to be answered.

CRedit author statement

Emma Versteegh: Methodology, Formal analysis, Investigation, Data Curation, Writing - Original Draft, Writing - Review & Editing, Visualization. **Cindy Van Dover:** Methodology, Investigation, Resources, Writing - Review & Editing. **Loïc Van Audenhaeghe:** Formal analysis, Visualization, Writing - Review & Editing. **Max Coleman:** Conceptualization, Methodology, Writing - Review & Editing, Supervision, Project administration, Funding acquisition.

Funding

This work was supported by the NASA Program, Astrobiology Science and Technology for Exploring Planets [grant number NNX09AB75G]; the Deep Carbon Observatory/Alfred P. Sloan Foundation; and the European Union's Horizon 2020 research and innovation project iAtlantic [grant number 818123]. This output reflects only the authors' view and the European Union cannot be held responsible for any use that may be made of the information contained therein. The funding sources had no role in study design, collection, analysis and interpretation of data, writing of the report, or the decision to submit the article for publication.

Declaration of competing interest

The authors declare that they have no known competing financial interests or personal relationships that could have appeared to influence the work reported in this paper.

Data availability

The data can be found at: Versteegh, Emma (2022), "Versteegh et al. *Rimicaris hybisae* CNS isotopes", Mendeley Data, V1, doi: [10.17632/6nvpw22zfk.1](https://doi.org/10.17632/6nvpw22zfk.1).

Acknowledgements

This research formed part of *Oases for Life* project. We would like to thank the crews of *E/V Nautilus* and its ROV *Hercules* team and of the *R/V Falkor* and the hybrid underwater robotic vehicle *Nereus* team, without whom this research would not have been possible. We thank the Schmidt Ocean Institute for the support of the *Oases 2013 Expedition* on the *R/V Falkor*. We also thank Kenneth Williford and Michael Tuite for their great help with C and N isotope analyses. We acknowledge suggestions of Loïc N. Michel for statistical analyses. The contributions of EAAV and MC were carried out at the Jet Propulsion Laboratory (JPL), California Institute of Technology, under contract with the National Aeronautics and Space Administration (NASA). We would like to thank two anonymous reviewers for their suggestions, which greatly helped improve the quality of this publication.

References

- Apremont, V., Cambon-Bonavita, M.-A., Cuffe-Gauchard, V., François, D., Pradillon, F., Corbari, L., Zbinden, M., 2018. Gill chamber and gut microbial communities of the hydrothermal shrimp *Rimicaris chacei* Williams and Rona 1986: a possible symbiosis. *PLoS One* 13 (11), e0206084. <https://doi.org/10.1371/journal.pone.0206084>.
- Assié, A., 2016. Deep Se(a)quencing: A Study of Deep-Sea Ectosymbioses Using Next Generation Sequencing. University of Bremen Bremen, Bremen.
- Bennett, S.A., Dover, C.V., Breier, J.A., Coleman, M., 2015. Effect of depth and vent fluid composition on the carbon sources at two neighboring deep-sea hydrothermal vent fields (Mid-Cayman Rise). *Deep Sea Res. Oceanogr. Res. Pap.* 104, 122–133. <https://doi.org/10.1016/j.dsr.2015.06.005>.
- Cavanaugh, C.M., Gardiner, S.L., Jones, M.L., Jannasch, H.W., Waterbury, J.B., 1981. Prokaryotic Cells in the hydrothermal vent tube Worm *Riftia pachyptila* Jones: possible chemoautotrophic symbionts. *Science* 213 (4505), 340–342. <https://doi.org/10.1126/science.213.4505.340>.
- Colaço, A., Dehairs, F., Desbruyères, D., 2002. Nutritional relations of deep-sea hydrothermal fields at the Mid-Atlantic Ridge: a stable isotope approach. *Deep Sea Res. Oceanogr. Res. Pap.* 49 (2), 395–412. [https://doi.org/10.1016/S0967-0637\(01\)00060-7](https://doi.org/10.1016/S0967-0637(01)00060-7).
- Colaço, A., Desbruyères, D., Guezennec, J., 2007. Polar lipid fatty acids as indicators of trophic associations in a deep-sea vent system community. *Mar. Ecol. Prog. Ser.* 348 (1), 15–24. <https://doi.org/10.1111/j.1439-0485.2006.00123.x>.
- Connelly, D.P., Copley, J.T., Murton, B.J., Stansfield, K., Tyler, P.A., German, C.R., Van Dover, C.L., Amon, D., Furlong, M., Grindlay, N., Hayman, N., Huhnerbach, V., Judge, M., Le Bas, T., McPhail, S., Meier, A., Nakamura, K.-i., Nye, V., Pebody, M., Pedersen, R.B., Plouviez, S., Sands, C., Searle, R.C., Stevenson, P., Taws, S., Wilcox, S., 2012. Hydrothermal vent fields and chemosynthetic biota on the world's deepest seafloor spreading centre. *Nat. Commun.* 3, 620. <https://doi.org/10.1038/ncomms1636>.
- Copley, J.T.P., Tyler, P.A., Murton, B.J., Van Dover, C.L., 1997. Spatial and interannual variation in the faunal distribution at Broken Spur vent field (29°N, Mid-Atlantic Ridge). *Mar. Biol.* 129 (4), 723–733. <https://doi.org/10.1007/s002270050215>.
- Corliss, J.B., Dymond, J., Gordon, L.I., Edmond, J.M., von Herzen, R.P., Ballard, R.D., Green, K., Williams, D., Bainbridge, A., Crane, K., van Andel, T.H., 1979. Submarine thermal springs on the Galápagos Rift. *Science* 203 (4385), 1073–1083. <https://doi.org/10.1126/science.203.4385.1073>.
- Cornwell, W.K., Schwillk, L.D., Ackerly, D.D., 2006. A trait-based test for habitat filtering: convex hull volume. *Ecology* 87 (6), 1465–1471. [https://doi.org/10.1890/0012-9658\(2006\)87\[1465:atthf\]2.0.co;2](https://doi.org/10.1890/0012-9658(2006)87[1465:atthf]2.0.co;2).
- Cowart, D.A., Durand, L., Cambon-Bonavita, M.-A., Arnaud-Haond, S., 2017. Investigation of bacterial communities within the digestive organs of the hydrothermal vent shrimp *Rimicaris exoculata* provide insights into holobiont geographic clustering. *PLoS One* 12 (3), e0172543. <https://doi.org/10.1371/journal.pone.0172543>.
- Cucherousset, J., Villéger, S., 2015. Quantifying the multiple facets of isotopic diversity: new metrics for stable isotope ecology. *Ecol. Indic.* 56, 152–160. <https://doi.org/10.1016/j.ecolind.2015.03.032>.
- DeNiro, M.J., Epstein, S., 1978. Influence of diet on the distribution of carbon isotopes in animals. *Geochem. Cosmochim. Acta* 42 (5), 495–506. [https://doi.org/10.1016/0016-7037\(78\)90199-0](https://doi.org/10.1016/0016-7037(78)90199-0).
- Durand, L., Roumagnac, M., Cuffe-Gauchard, V., Jan, C., Guri, M., Tessier, C., Haond, M., Crassous, P., Zbinden, M., Arnaud-Haond, S., Cambon-Bonavita, M.-A., 2015. Biogeographical distribution of *Rimicaris exoculata* resident gut epibiont communities along the Mid-Atlantic Ridge hydrothermal vent sites. *FEMS (Fed. Eur. Microbiol. Soc.) Microbiol. Ecol.* 91 (10) <https://doi.org/10.1093/femsec/fiv101>.
- Durand, L., Zbinden, M., Cuffe-Gauchard, V., Duperron, S., Roussel, E.G., Shillito, B., Cambon-Bonavita, M.-A., 2009. Microbial diversity associated with the hydrothermal shrimp *Rimicaris exoculata* gut and occurrence of a resident microbial community. *FEMS (Fed. Eur. Microbiol. Soc.) Microbiol. Ecol.* 71 (2), 291–303. <https://doi.org/10.1111/j.1574-6941.2009.00806.x>.
- Fry, B., Arnold, C., 1982. Rapid ¹³C/¹²C turnover during growth of brown shrimp (*Penaeus aztecus*). *Oecologia* 54 (2), 200–204. <https://doi.org/10.1007/BF00378393>.
- Gebruk, A.V., Southward, E.C., Kennedy, H., Southward, A.J., 2000. Food sources, behaviour, and distribution of hydrothermal vent shrimps at the Mid-Atlantic Ridge. *J. Mar. Biol. Assoc. U. K.* 80 (3), 485–499. <https://doi.org/10.1017/S0025315400002186>.
- German, C.R., Bowen, A., Coleman, M.L., Honig, D.L., Huber, J.A., Jakuba, M.V., Kinsey, J.C., Kurz, M.D., Leroy, S., McDermott, J.M., de Lépinay, B.M., Nakamura, K., Seewald, J.S., Smith, J.L., Sylva, S.P., Van Dover, C.L., Whitcomb, L. L., Yoerger, D.R., 2010. Diverse styles of submarine venting on the ultraslow spreading Mid-Cayman Rise. *Proc. Natl. Acad. Sci. USA* 107 (32), 14020–14025. <https://doi.org/10.1073/pnas.1009205107>.
- Hernández-Ávila, I., Cambon-Bonavita, M.-A., Sarrazin, J., Pradillon, F., 2022. Population structure and reproduction of the alvinocaridid shrimp *Rimicaris exoculata* on the Mid-Atlantic Ridge: variations between habitats and vent fields. *Deep Sea Res. Oceanogr. Res. Pap.* 186, 103827 <https://doi.org/10.1016/j.dsr.2022.103827>.
- Hesslein, R.H., Hallard, K.A., Ramlal, P., 1993. Replacement of sulfur, carbon, and nitrogen in tissue of growing broad Whitefish (*Coregonus nasus*) in response to a change in diet traced by δ³⁴S, δ¹³C, and δ¹⁵N. *Can. J. Fish. Aquat. Sci.* 50 (10), 2071–2076. <https://doi.org/10.1139/f93-230>.
- Hügler, M., Petersen, J.M., Dubilier, N., Imhoff, J.F., Sievert, S.M., 2011. Pathways of carbon and energy metabolism of the epibiotic community associated with the deep-sea hydrothermal vent shrimp *Rimicaris exoculata*. *PLoS One* 6 (1), e16018. <https://doi.org/10.1371/journal.pone.0016018>.
- Jan, C., Petersen, J.M., Werner, J., Teeling, H., Huang, S., Glöckner, F.O., Golyshina, O. V., Dubilier, N., Golyshin, P.N., Jebbar, M., 2014. The gill chamber epibiosis of deep-sea shrimp *Rimicaris exoculata*: an in-depth metagenomic investigation and discovery of Zetaproteobacteria. *Environ. Microbiol.* 16 (9), 2723–2738. <https://doi.org/10.1111/1462-2920.12406>.
- Kennicutt, M.C., Burke Jr., R.A., MacDonald, I.R., Brooks, J.M., Denoux, G.J., Macko, S. A., 1992. Stable isotope partitioning in seep and vent organisms: chemical and ecological significance. *Chem. Geol. Isot. Geosci.* 101 (3–4), 293–310. [https://doi.org/10.1016/0009-2541\(92\)90009-1](https://doi.org/10.1016/0009-2541(92)90009-1).
- Kinsey, J.C., German, C.R., 2013. Sustained volcanically-hosted venting at ultraslow ridges: Piccard hydrothermal field, Mid-Cayman Rise. *Earth Planet Sci. Lett.* 380, 162–168. <https://doi.org/10.1016/j.epsl.2013.08.001>, 0.
- Leonard, J.M., Mitchell, J., Beinart, R.A., Delaney, J.A., Sanders, J.G., Ellis, G., Goddard, E.A., Girguis, P.R., Scott, K.M., Atomi, H., 2021. Cooccurring Activities of two autotrophic pathways in symbionts of the hydrothermal vent tubeworm *Riftia pachyptila*. *Appl. Environ. Microbiol.* 87 (17) <https://doi.org/10.1128/AEM.00794-21.e00794-00721>.
- Lonsdale, P., 1977. Clustering of suspension-feeding macrobenthos near abyssal hydrothermal vents at oceanic spreading centers. *Deep-Sea Res.* 24 (9), 857–863. [https://doi.org/10.1016/0146-6291\(77\)90478-7](https://doi.org/10.1016/0146-6291(77)90478-7).
- McCutchan, J.H., Lewis, W.M., Kendall, C., McGrath, C.C., 2003. Variation in trophic shift for stable isotope ratios of carbon, nitrogen, and sulfur. *Oikos* 102 (2), 378–390. <https://doi.org/10.1034/j.1600-0706.2003.12098.x>.
- Methou, P., Hernández-Ávila, I., Cathalot, C., Cambon-Bonavita, M.A., Pradillon, F., 2022. Population structure and environmental niches of *Rimicaris* shrimps from the Mid-Atlantic Ridge. *Mar. Ecol. Prog. Ser.* 684, 1–20. <https://doi.org/10.3354/meps13986>.

- Methou, P., Michel, L.N., Segonzac, M., Cambon-Bonavita, M.-A., Pradillon, F., 2020. Integrative taxonomy revisits the ontogeny and trophic niches of *Rimicaris* vent shrimps. *R. Soc. Open Sci.* 7 (7), 200837 <https://doi.org/10.1098/rsos.200837>.
- Minagawa, M., Wada, E., 1984. Stepwise enrichment of ^{15}N along food chains: further evidence and the relation between $\delta^{15}\text{N}$ and animal age. *Geochem. Cosmochim. Acta* 48 (5), 1135–1140. [https://doi.org/10.1016/0016-7037\(84\)90204-7](https://doi.org/10.1016/0016-7037(84)90204-7).
- Nye, V., Copley, J., Linse, K., Plouviez, S., 2013a. *Iheyaspira bathycodon* new species (Vetigastropoda: Trochoidea: Turbinidae: Skeneinae) from the Von Damm vent field, Mid-Cayman spreading centre, Caribbean. *J. Mar. Biol. Assoc. U. K.* 93 (4), 1017–1024. <https://doi.org/10.1017/S0025315412000823>.
- Nye, V., Copley, J., Plouviez, S., 2012. A new species of *Rimicaris* (Crustacea: Decapoda: Caridea: Alvinocarididae) from hydrothermal vent fields on the Mid-Cayman spreading centre, Caribbean. *J. Mar. Biol. Assoc. U. K.* 92 (5), 1057–1072. <https://doi.org/10.1017/S0025315411002001>.
- Nye, V., Copley, J.T., Tyler, P.A., 2013b. Spatial variation in the population structure and reproductive biology of *Rimicaris hybisae* (Caridea: Alvinocarididae) at hydrothermal vents on the Mid-Cayman Spreading Centre. *PLoS One* 8 (3), e60319. <https://doi.org/10.1371/journal.pone.0060319>.
- Petersen, J.M., Zielinski, F.U., Pape, T., Seifert, R., Moraru, C., Amann, R., Hourdez, S., Girguis, P.R., Wankel, S.D., Barbe, V., Pelletier, E., Fink, D., Borowski, C., Bach, W., Dubilier, N., 2011. Hydrogen is an energy source for hydrothermal vent symbioses. *Nature* 476 (7359), 176–180. <https://doi.org/10.1038/nature10325>.
- Plouviez, S., Jacobson, A., Wu, M., Van Dover, C.L., 2015. Characterization of vent fauna at the Mid-Cayman spreading center. *Deep Sea Res. Oceanogr. Res. Pap.* 97, 124–133. <https://doi.org/10.1016/j.dsr.2014.11.011>.
- Polz, M.F., Robinson, J.J., Cavanaugh, C.M., Van Dover, C.L., 1998. Trophic ecology of massive shrimp aggregations at a Mid-Atlantic Ridge hydrothermal vent site. *Limnol. Oceanogr.* 43 (7), 1631–1638. <https://doi.org/10.4319/lo.1998.43.7.1631>.
- Pond, D., Dixon, D., Bell, M., Fallick, A., Sargent, J., 1997. Occurrence of 16: 2 (n-4) and 18: 2 (n-4) fatty acids in the lipids of the hydrothermal vent shrimps *Rimicaris exoculata* and *Alvinocaris markensis*: nutritional and trophic implications. *Mar. Ecol. Prog. Ser.* 156, 167–174. <https://doi.org/10.3354/meps156167>.
- Ponsard, J., Cambon-Bonavita, M.-A., Zbinden, M., Lepoint, G., Joassin, A., Corbari, L., Shillito, B., Durand, L., Cueff-Gauchard, V., Compère, P., 2013. Inorganic carbon fixation by chemosynthetic ectosymbionts and nutritional transfers to the hydrothermal vent host-shrimp *Rimicaris exoculata*. *ISME J.* 7 (1), 96–109. <https://doi.org/10.1038/ismej.2012.87>.
- R Core Team, 2013. *R: A Language and Environment for Statistical Computing*.
- Rieley, G., Dover, C.L.V., Hedrick, D.B., Eglinton, G., 1999. Trophic ecology of *Rimicaris exoculata*: a combined lipid abundance/stable isotope approach. *Mar. Biol.* 133 (3), 495–499. <https://doi.org/10.1007/s002270050489>.
- Segonzac, M., de Saint-Laurent, M., Casanova, B., 1993. L'énigme du comportement trophique des crevettes Alvinocarididae des sites hydrothermaux de la dorsale médio-atlantique. *Cah. Biol. Mar.* 34 (4), 535–571.
- Streit, K., Bennett, S.A., Van Dover, C.L., Coleman, M., 2015. Sources of organic carbon for *Rimicaris hybisae*: tracing individual fatty acids at two hydrothermal vent fields in the Mid-Cayman Rise. *Deep Sea Res. Oceanogr. Res. Pap.* 100, 13–20. <https://doi.org/10.1016/j.dsr.2015.02.003>.
- Suh, Y.J., Kim, M.-S., Kim, S.-J., Kim, D., Ju, S.-J., 2022. Carbon sources and trophic interactions of vent fauna in the Onnuri Vent Field, Indian Ocean, inferred from stable isotopes. *Deep Sea Res. Oceanogr. Res. Pap.* 182, 103683 <https://doi.org/10.1016/j.dsr.2021.103683>.
- Teixeira, S., Olu, K., Decker, C., Cunha, R.L., Fuchs, S., Hourdez, S., Serrão, E.A., Arnaud-Haond, S., 2013. High connectivity across the fragmented chemosynthetic ecosystems of the deep Atlantic Equatorial Belt: efficient dispersal mechanisms or questionable endemism? *Mol. Ecol.* 22 (18), 4663–4680. <https://doi.org/10.1111/mec.12419>.
- Turner, T.F., Collyer, M.L., Krabbenhoft, T.J., 2010. A general hypothesis-testing framework for stable isotope ratios in ecological studies. *Ecology* 91 (8), 2227–2233. <https://doi.org/10.1890/09-1454.1>.
- Van Dover, C.L., 2002. Trophic relationships among invertebrates at the Kairei hydrothermal vent field (Central Indian Ridge). *Mar. Biol.* 141 (4), 761–772. <https://doi.org/10.1007/s00227-002-0865-y>.
- Van Dover, C.L., Fry, B., Grassle, J.F., Humphris, S., Rona, P.A., 1988. Feeding biology of the shrimp *Rimicaris exoculata* at hydrothermal vents on the Mid-Atlantic Ridge. *Mar. Biol.* 98 (2), 209–216. <https://doi.org/10.1007/BF00391196>.
- Vander Zanden, M.J., Rasmussen, J.B., 2001. Variation in $\delta^{15}\text{N}$ and $\delta^{13}\text{C}$ trophic fractionation: implications for aquatic food web studies. *Limnol. Oceanogr.* 46 (8), 2061–2066. <https://doi.org/10.4319/lo.2001.46.8.2061>.
- Vereshchaka, A.L., Kulagin, D.N., Lunina, A.A., 2015. Phylogeny and new Classification of hydrothermal vent and seep shrimps of the family Alvinocarididae (Decapoda). *PLoS One* 10 (7), e0129975. <https://doi.org/10.1371/journal.pone.0129975>.
- Vereshchaka, A.L., Vinogradov, G.M., Lein, A.Y., Dalton, S., Dehairs, F., 2000. Carbon and nitrogen isotopic composition of the fauna from the Broken Spur hydrothermal vent field. *Mar. Biol.* 136 (1), 11–17. <https://doi.org/10.1007/s002270050002>.
- Vetter, R.D., Fry, B., 1998. Sulfur contents and sulfur-isotope compositions of thiotrophic symbioses in bivalve molluscs and vestimentiferan worms. *Mar. Biol.* 132 (3), 453–460. <https://doi.org/10.1007/s002270050411>.
- Villéger, S., Novack-Gottshall, P.M., Mouillot, D., 2011. The multidimensionality of the niche reveals functional diversity changes in benthic marine biotas across geological time. *Ecol. Lett.* 14 (6), 561–568. <https://doi.org/10.1111/j.1461-0248.2011.01618.x>.
- Vinogradov, M., Vereshchaka, A., 1995. The micro-scale distribution of the hydrothermal near-bottom shrimp fauna. *Deep Sea Newsl.* 23, 18–21.
- Vinogradsky, S., 1887. Über Schwefelbakterien. *Botanische Zeitung* 45, 489–610.
- Zbinden, M., Cambon-Bonavita, M.-A., 2003. Occurrence of deferritbacteriales and entomoplasmatales in the deep-sea Alvinocarid shrimp *Rimicaris exoculata* gut. *FEMS (Fed. Eur. Microbiol. Soc.) Microbiol. Ecol.* 46 (1), 23–30. [https://doi.org/10.1016/S0168-6496\(03\)00176-4](https://doi.org/10.1016/S0168-6496(03)00176-4).
- Zbinden, M., Cambon-Bonavita, M.A., 2020. *Rimicaris exoculata*: biology and ecology of a shrimp from deep-sea hydrothermal vents associated with ectosymbiotic bacteria. *Mar. Ecol. Prog. Ser.* 652, 187–222. <https://doi.org/10.3354/meps13467>.
- Zbinden, M., Shillito, B., Le Bris, N., de Villardi de Montlaur, C., Roussel, E., Guyot, F., Gaill, F., Cambon-Bonavita, M.-A., 2008. New insights on the metabolic diversity among the epibiotic microbial community of the hydrothermal shrimp *Rimicaris exoculata*. *J. Exp. Mar. Biol. Ecol.* 359 (2), 131–140. <https://doi.org/10.1016/j.jembe.2008.03.009>.